Romanian Journal of Mechanics
Volume 4, Issue 2/2019, pp 15-28, ISSN 2537 - 5229, rjm.journals.srmta.ro

ADVANCES IN NON-SURGICAL MANAGEMENT OF LIVER TUMOR

Rodica IOAN [*,**] , **Ligia MUNTEANU** [*] , **Iulian GIRIP** [*]

[*] Institute of Solid Mechanics, Romanian Academy

[**] University Spiru Haret, Bucharest

Corresponding author: Rodica IOAN, E-mail: rodicaioan08@yahoo.com

Abstract The robotic-assisted liver tumor therapy by targeted delivery of drugs into the tumor is an innovative technique applied in the case of nonresectable tumors. It is difficult for the surgeon to perform by himself the surgical plan because of some major difficulties which may occur during the procedure, such as the insertion trajectory of the needle can touch the ribs, blood vessels and other tissues and organs in the vicinity of the liver, or the inserted needle may cause deformation of liver which can change the map of the tumor surroundings. Thus, an effective surgical plan is needed. To overcome these difficulties the optimization of the needle free-collision trajectories is performed by using the particle swarm optimization algorithm. The paper was presented to the International Multi-Conference on Systems & Structures (SysStruc '19), Reșița, November 7-9, 2019.

Key words: Minimally invasive surgery, Trajectory optimization, Particle swarm optimization

1. INTRODUCTION

Th e history of liver surgery originates in antiquity. The Babylonian, Egyptian, Greek and Roman societies papers considered the liver as the noble organ, the organ of life because it contains the most blood.

Over the past decade, the targeted delivery of drugs into the liver tumors, as a minimally invasive surgery, has been used extensively in the liver tumor treatments due to its safety, rapid recovery, and low cost [1-3]. In this technique, two important points must stand in the surgeon's attention: tumor size and accessibility.

The medical imaging is used localization of the liver tumors- magnetic resonance, computerized Tomography, digital radiology, etc. The challenge arises especially for the surgeon who has to place correctly and precisely the incision point on the skin.

Accurate location of the incision must allow minimal local damages by avoiding the ribs, blood vessels and other tissues and organs in liver vicinity and also, not exceeding the length of the needle.

Most methods are based on virtual reality (VR) and on the detection of the collision between needles and obstacles. Shaoli *et al*. [4] introduced a surgical method with multiple needles and calculated point by point the optimal trajectories in order to avoid collision with obstacles.

Cristina et al. [5] presented a system for the generation of personalized biomodels of patients in VR, based on the analysis and segmentation of the medical image. Butnariu *et al*. [6] presented a VR-based method to generate and optimize the needle trajectory in the robotic brachytherapy procedure. Schumann *et al*. [7] presented a visualization method for choosing the best 2D slice

trajectory. Shamir *et al*. [8] have presented a method by which the surgeon can select a trajectory using a 3D visualization map of the abdominal area.

Although these methods are beneficial for the surgeon in deciding the needle or multiple needle trajectories, they are still highly dependent on the surgeon's skills and experience, and determining and planning the optimal trajectories to the target are not developed.

For this reason, Villard *et al*. [6] proposed a force feedback haptic to obtain the optimal needle incision position. Seitel [9] noticed that the method did not give as good results as expected because of the very long execution time and the difficulty in determining the optimal parameters for each new tumor shape in individual patients.

To reduce the dependence on surgeon's skill, the concept of *virtual fixture* (VF) [10, 11] has been adopted in surgical planning. The present paper refers to the optimization of the collision-free trajectory of the surgical needle who is carrying drugs into the tumoral target, with fulfillment of all surgical constraints. The reconstruction of the collision-free workspace and the possible needle insertion areas, as well as the collision-free trajectories chosen by the surgeon and verified by the robot are analyzed in order to eliminate the invalid insertion points (Fig. 1).

The rigid needle is not suitable for all cases. Sometimes is needed a flexible and soft needle do not damage the tissues, especially when the tumors lie in the critical area of hepatic vessels [12, 13].

As for the rigid needles, the flexible needles know some shortcomings appear. It is difficult to find an optimal trajectory in which the needle can arrive to the tumors without damaging the neighboring organs and vessels. Also, the pushing force and angle cannot control the flexible needles free of more controlling parameters such as the screwing force. The spatial controllability of flexible needles is not clear yet. Till now the research is based on computer simulations of homogeneous materials. The optimal trajectories for flexible needles are more frequently modeled as inverse problems. The optimal trajectory is finding by watching the needle progressing, followed by computing some control parameters in accordance with the motion, the properties of flexible needles and the soft tissues.

The optimization problem proposed in this article aims to determine the free of collision optimal trajectory of the surgical needle in the conditions of fulfilling some performance indicators for the robot. The particle swarm optimization algorithm is applied to solve this optimization problem [14, 15].

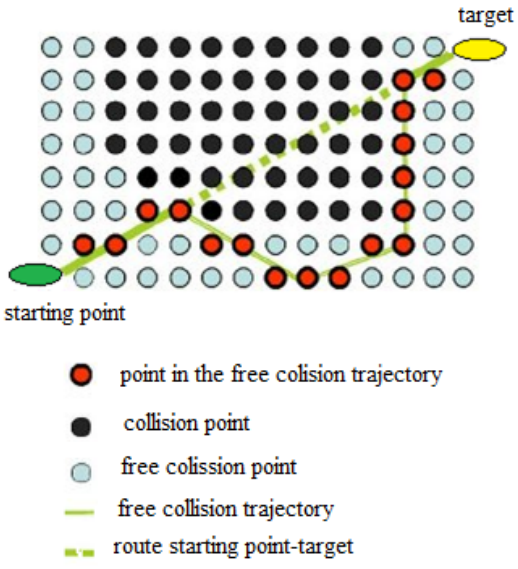

Fig. 1. Free collision trajectories.

2. PROBLEM FORMULATION

The goal of the robot is to stop the needle to cross the critical boundaries and helping the surgeon to resolve conflicting trajectories towards the tumor (Figure 2). The contact (a possible collision point) between the needle and the tissue is analyzed by an identifier to check the minimum distance between needle and the surrounding tissue [15]. The minimum distance is expressed as

$$\min\left(\frac{1}{2}(r_1 - r_2)^T (r_1 - r_2)\right), \tag{1}$$

with $f_1(r_1) \le 0$, $f_2(r_2) \le 0$, r_1, r_2, the position vectors of two points belonging to the needle and the tissue, respectively, and f_1, f_2, the surfaces to the needle and the tissue, respectively. The interference distance or penetration is defined as

$$\min(-d), \quad f_1(r_1) \le -\frac{d}{2}, \quad f_2(r_2) \le -\frac{d}{2}, \tag{2}$$

where d is the penetration.

The position of the tumor and a possible needle trajectory is shown in Fig. 2.

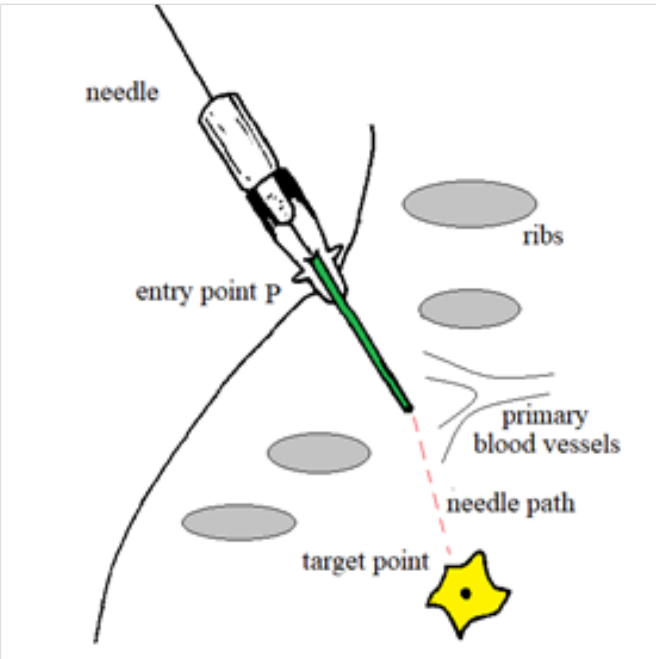

Fig. 2. The position of the tumor and a possible needle trajectory.

The position of a collision point is determined with respect to an arbitrary system of coordinates. After its detection, a modified trajectory is created. The original trajectory is modified using distinct points as shown in Fig. 3.

As application, we consider the case of a tumor with a difficult location, in the vicinity of the portal tree of the vascular territory in the liver (Fig. 4a).

The trajectory of the needle is established by the surgeon through the analyses of the microscope image (Fig. 4a) [18]. White and grey denote forbidden areas while the shade of purple are safe regions. The tumor is drawn in red and the green line is the proposed safe trajectory.

The detection allows for feedback to the trajectories planning and obtaining the global avoidance (Fig. 5).

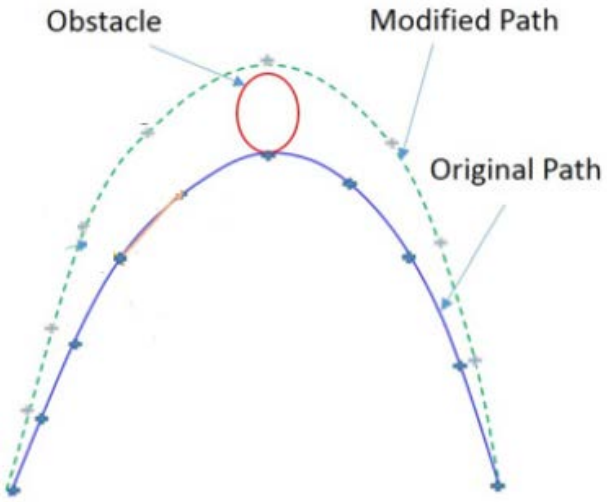

Fig. 3**.** Modification of path for collision avoidance.

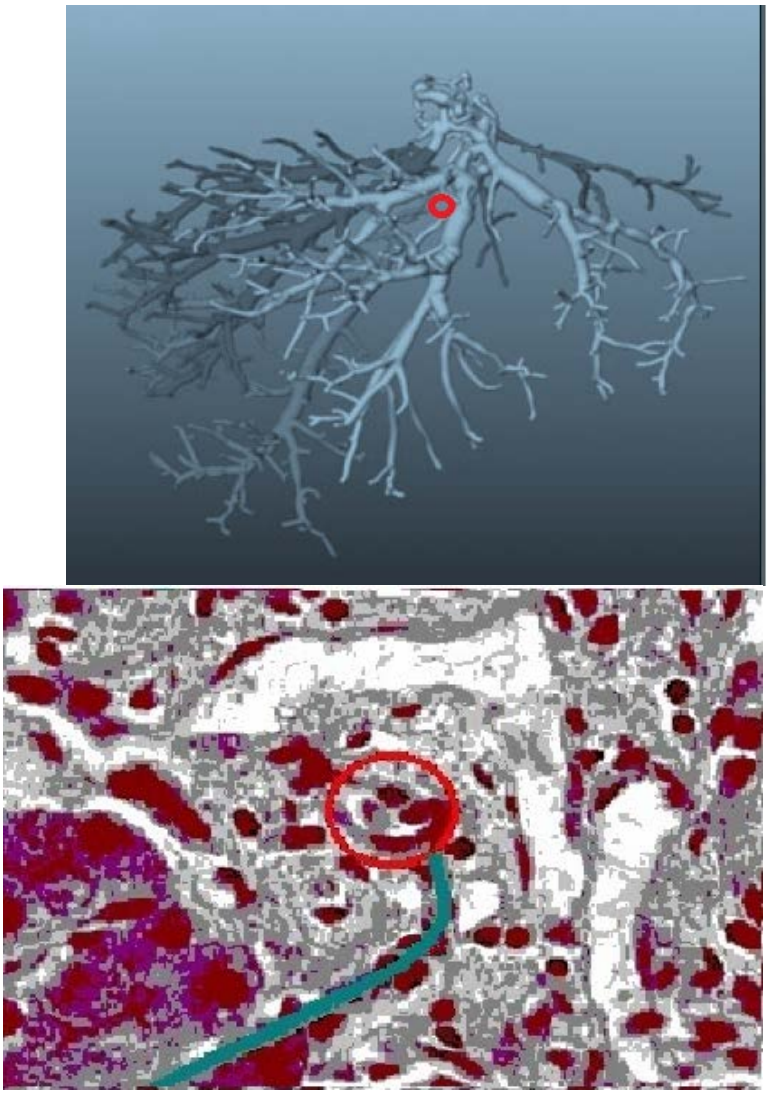

Fig.4. a) Location of the tumor; b) Tumor image seen on the microscope.

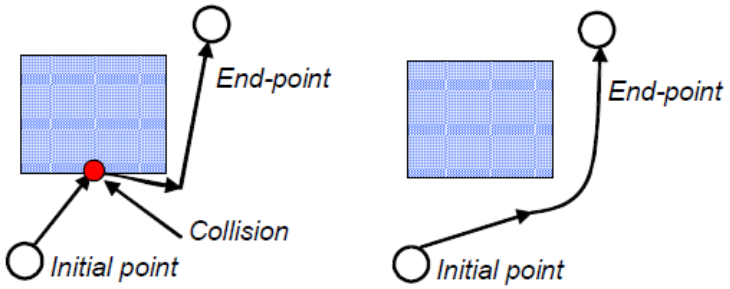

Fig. 5. Local and global avoidance of collisions.

The scenario of finding the free-collision trajectory is expressed as a multi-objective problem that assumes a number of n objective functions $f_1(x), f_2(x),..., f_d(x)$, and d decision variables $x = (x_1, x_2,..., x_d)^T$.

The algorithm finds the set region $R \subseteq R^d$ of vectors x, where $x \in R^d$ in order to

Maximise

$$y = F(x) = (f_1(x), f_2(x),..., f_d(x))^T, \quad x \in S, \tag{3}$$

$$F : S \to Y, \quad Y = \{F(x) \mid x \in S\}, \tag{4}$$

$$x = (x_1, x_2,..., x_d)^T, \tag{5}$$

where $f_i(x)$, $i = 1,2,...,n$ are n objective functions, and $(x_1, x_2,..., x_d)$ are d decision variables and n the optimization parameters. $S \in \mathrm{R}^n$ is the parameter space, and $Y \in \mathrm{R}^k$ is referred as an attribute space, F is a nonlinear function, and S is defined by constraints containing both continuous and discrete variables.

The objective functions are defined by the *target heading*, *clearance* and some robotic performance such as *dexterity index*, *manipulability index*, *the Jacobian condition number* and *the minimum singular value* [14, 19].

The *target heading* is a measure of progress towards the target location. It is maximal if the needle moves directly towards the target. The *clearance* is the distance to the closest obstacle on the trajectory. The smaller the distance to an obstacle the higher is the robot's desire to move around it.

The performance index *dexterity* describes the robot mobility within the workspace. It is related to mobility of closed chain mechanisms, which may to be understood in relation to the link lengths. Grashof considered a four-link kinematic chain denoted by l, p, q and s. The shortest and the longest link lengths are s and l with $l > p \geq q > s$ [20]. Grashof stated that there exists at least one link which can rotate with respect to the other three links if

$$l + s \leq p + q, \tag{6}$$

and none of the four links can rotate if

$$l + s > p + q \ . \tag{7}$$

The rule (9) is known as the Grashof's criterion. The dexterity index $d \in [0,1]$ is defined as

$$d = \frac{d_x + d_y + d_z}{3}, \tag{8}$$

where d_x, d_y, d_z are indices in directions X, Y, Z defined as

$$d_x = -\frac{\Delta\alpha}{2\pi},\ d_y = -\frac{\Delta\beta}{2\pi},\ d_z = -\frac{\Delta\gamma}{2\pi}, \tag{9}$$

where Δ measures a possible variation of the angle for each point in the workspace.

The dexterity index takes values in the range $[0,1]$ because it is impossible for a robot to have the same dexterity index at all points in the workspace. If $d = 1$ the manipulator has full dexterity at a particular point or area.

The manipulability index measures the ability to arbitrarily change the position and orientation of the end-effector. If θ is the join coordinate vector of the robot, the relationship between the position of the end-effector p and θ is

$$J\theta = p, \tag{10}$$

where J is the Jacobean matrix of the robot.

The orientation in a given point in the workspace is represented by Euler angle yaw, pitch and roll angles. The manipulability index μ is defined as

$$\mu = \sqrt{\det(JJ^T)}, \tag{11}$$

being proportional to the volume of the ellipsoid of velocities. The manipulability index μ is zero in singular configurations.

The *Jacobian condition number* or *the isotropy index* is a performance index related to a better use of revolute-jointed six-degree-of-freedom serial robots in five-axis machining. This index has a kinetostatic nature and less dynamic because the frequency dynamic effects are not relevant to its variation. When $\det J = 0$, the robot approaches singularities. The condition number is a measure of Jacobian invertibility

$$k(J) = \| J \| \| J^{-1} \| \ ,\ \| J \| = \sqrt{\mathrm{tr}(JWJ)^T}\ ,$$

$$W = \frac{1}{\dim(J)} I\ , \tag{12}$$

for a square matrix J, and

$$k(J) = \frac{\sigma_{\max}}{\sigma_{\min}}\ , \tag{13}$$

with $\sigma_{\max}$ and $\sigma_{\min}$ are the maximum and minimum singular values of J. The definition (13) is valid only when the elements of J has the same units.

In the opposite case, it is possible to define a homogenous matrix by dividing the lines of J corresponding to the positions by characteristic length of the studied robot.

A Jacobian matrix unit is thus obtained. In the optimum design, the link lengths are adjusted so that the robot has maximum dexterity and maximum manipulability in the region of interest and maximum Jacobean condition number.

The performance indexes are measures of the kinematic capabilities of robots. Also, they are measures for design and control of kinematically redundant manipulators allowing comparison with other performance indexes in humans and machines.

3. PROBLEM SOLUTION

The particle swarm optimization algorithm is inspired also from nature. It is a stochastic optimization technique and it simulates the behavior of birds flocking and fish schooling. This algorithm is an evolutionary algorithm that searches the best solution by updating the current population. The members of the swarm *communicate* each member being aware of the best position among them. There are no operators as crossover, mutation or selection processes as in genetic algorithms. There are few references that use the Particle Swarm Algorithms to optimize the end-effector trajectories.

One example is to use this algorithm to the minimization of the stiffness over a cubic usable workspace of the structure of a parallel robot [21]. We must specify that, during Particle Swarm Algorithms, the simulator changes information continuously with the optimizer. The optimizer is tracking its algorithm of particle swarm and defines some points in the space of solutions and it submits, one by one, these solution-candidates to the simulator that receives and interprets them as the entry parameters for the simulation.

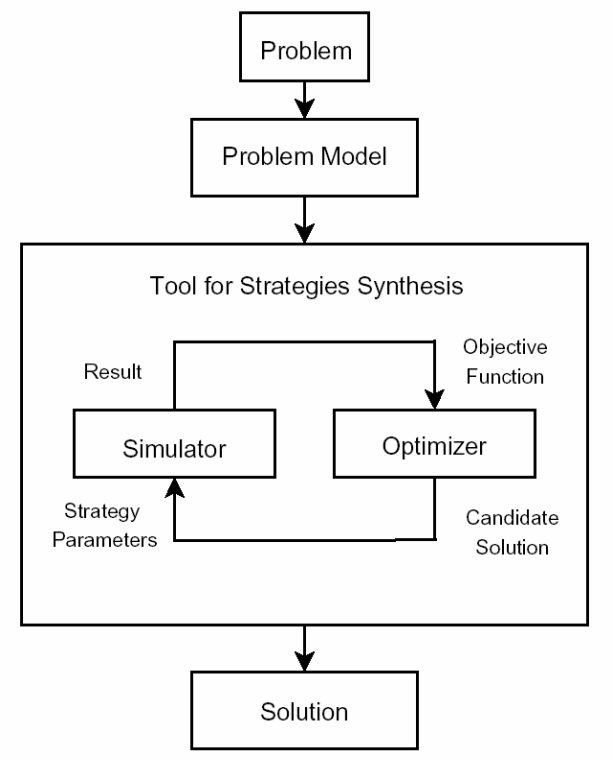

Fig.6. Optimization flow diagram.

At the end of the simulation, the outcomes of this are sent back to the optimizer, which interprets this information as the objective function of the solution-candidate that had been sent. It processes this information inside the algorithm routine and sends the next solution candidate, restarting a cycle that only ends when the optimizer finds some of its stopping criteria. Figure 6 shows the optimization flow diagram.

In the optimization of the free-collision trajectories appear often scenarios like those presented in Fig. 7, which cannot be solved by the genetic algorithm.

The optimization procedure can experience long periods of evolutionary inactivity interrupted by sudden, localized, and rapid evolutions. In these situations, the populations explore neutral solutions, and suddenly, a relevant change in the algorithm leads to a better solution. In Fig. 7a, a

premature convergence is depicted and the solution is drawn to a local optimum from which it cannot escape anymore. Fig. 7b shows a small neural bridge to the global optimum.

The optimization has a chance to escape the smaller peak if it is able to find the bridge, and in this way the chance to find the optimumhas increased. If this bridge is wider, as shown in Fig. 7c, the chance of finding the global optimum increases as well.

To allow the evaluation of the current position (x, y, z) of the needle, the algorithm uses introduced the equation

$$Eval. = \sqrt{(x-100)^2} + \sqrt{(y-100)^2} + \sqrt{(z-100)^2}, \tag{14}$$

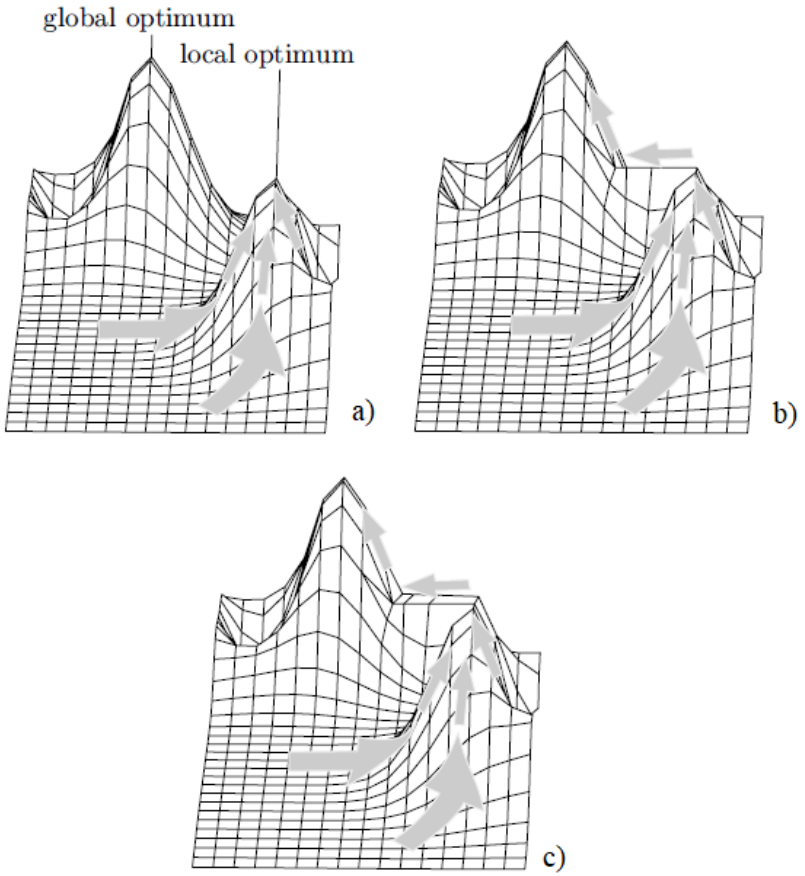

Fig. 7. (a) premature convergence; b) small neutral bridge and c) wide neutral bridge.

As such, (100,100) is the target. The optimization has been implemented in Matlab, using the Global Optimization Toolbox. In order to decrease the computational time, all the equation has been implemented in a vectorial manner.

The optimal solution and the improved solution obtained by solving the premature convergence and a wide neutral bridge cases are presented in Fig. 8. The evolution of the fitness value of the optimization is presented in Fig. 9 and the final value is $fit = 0.2113$. The algorithm has passed through 98 iterations until the final solution has been achieved. A population of 200 members has been used

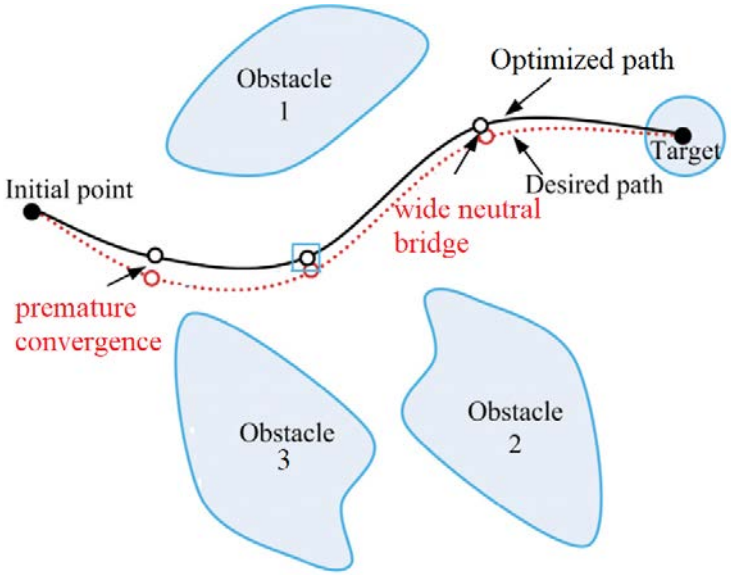

Fig. 8. The optimized and the desired paths in the cases of premature convergence and a wide neural bridge.

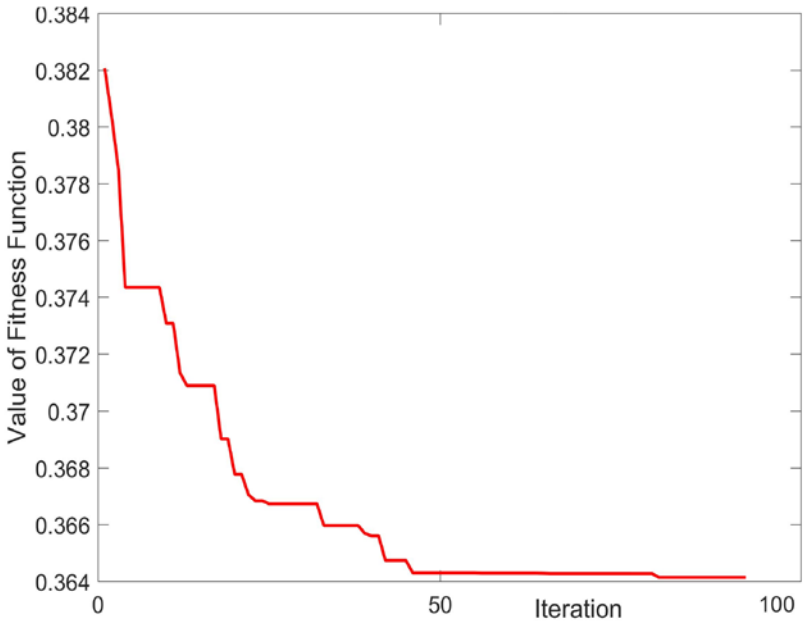

Fig. 9. Convergence of the objective function.

The critical points or frontiers are described by nonlinear boundary conditions for example, the vascular territories, the portal vein, the hepatic veins, the hepatic artery and the bile duct system near the critical domain. Near the critical points or frontiers or tumor the needle can oscillate.

The optimized free of collision trajectory is presented in Fig.10.

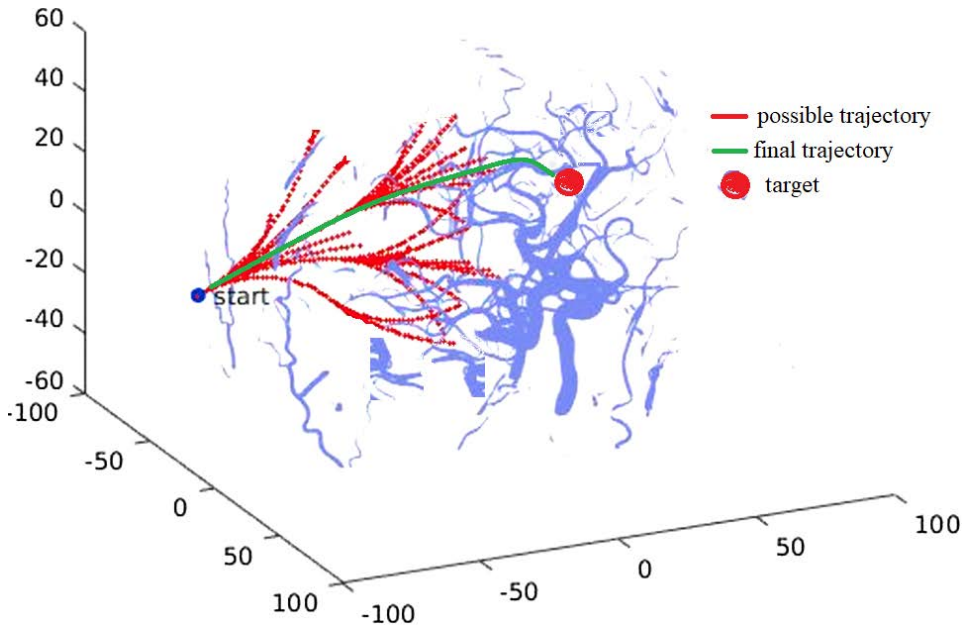

Fig. 10. The optimized free collision trajectory.

The coordinates of the needle are tracked during simulation and comparison between the desired and the actual trajectory are done in Fig. 11. The acceptable differences in accuracy between desired and actual trajectories are 0.12mm vesus 0.1 mm. The error norm graphic is shown in Fig.12.

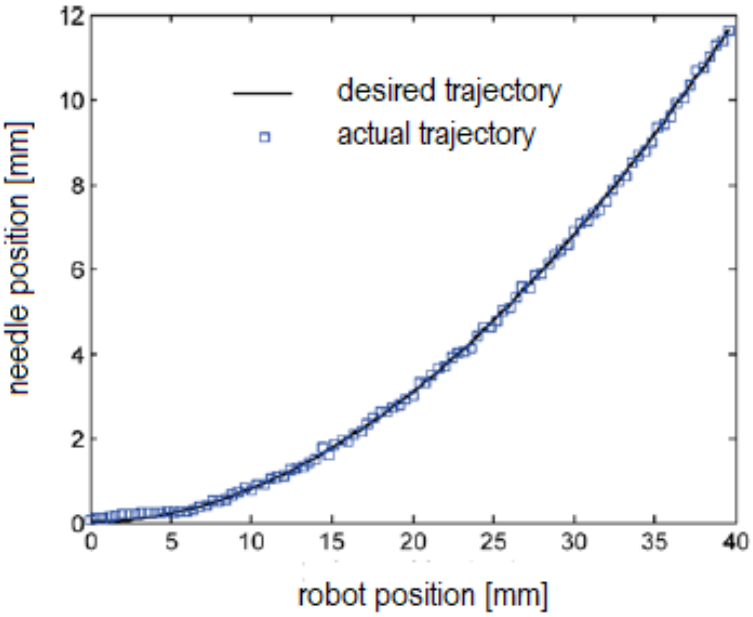

Fig.11. Trajectory tracking.

We tried to simulate the case of a tumor for which the needle moves through vibrations with important amplitudes. The obtaining of the optimal trajectory of the needle and its manipulation is an inverse kinematics problem starting from a given the position and orientation of the needle trajectory, the translation and orientation of the needle modeled as a function of needle progress into the tissue. The avoiding of obstacles while applying minimal lateral pressure on the tissue is a complex issue related to the minimal curvature of the needle and the presence of vibrations. The

trajectory problem can be reduced to finding the shortest curve that connects the tumor with the needle insertion point, and which avoids the obstacle by a predetermined distance while maintaining minimal needle curvature.

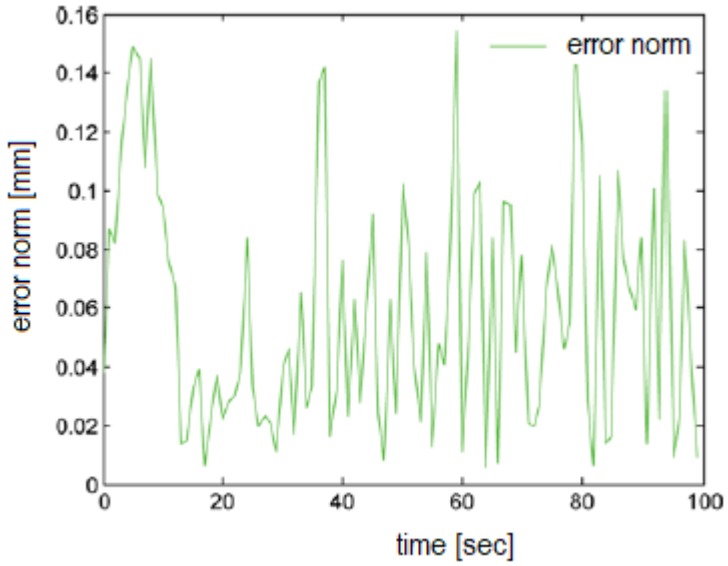

Fig. 12. Error norm graphic.

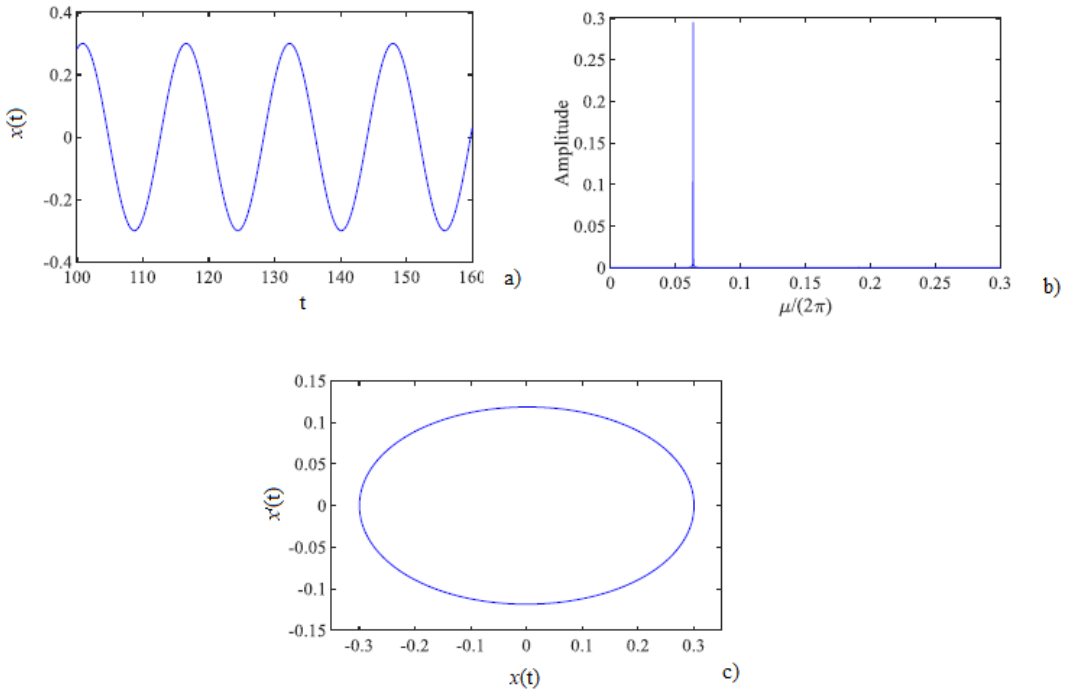

Fig.13. The stable and unstable needle trajectories simulation.

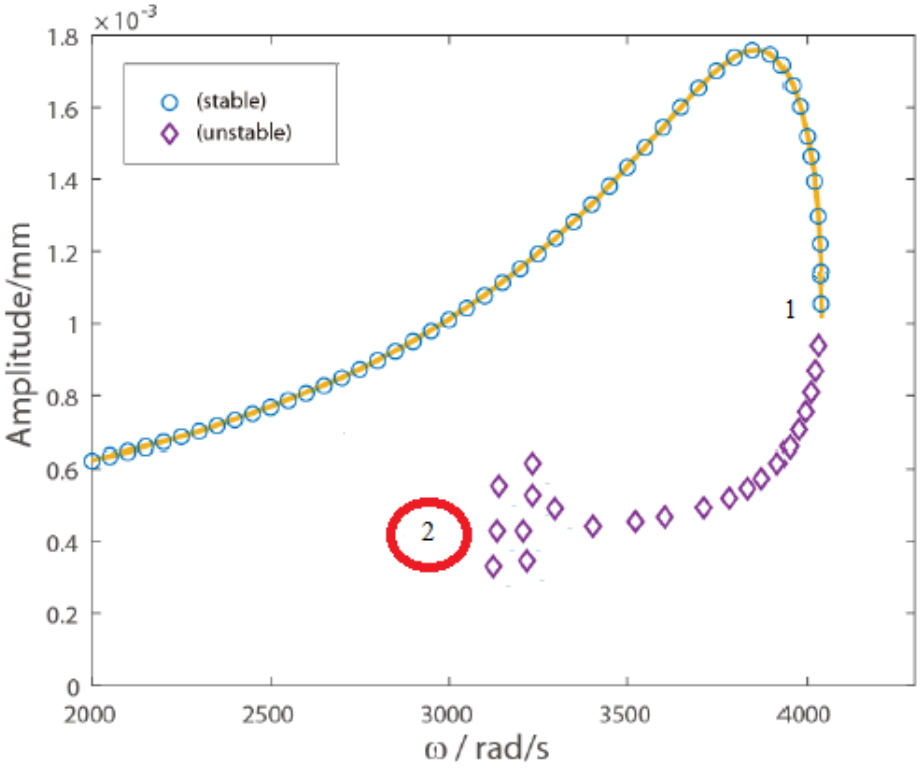

Fig.14. (a) The harmonic vibrations of the needle; b) the resonance, and c) the phase portrait of the needle trajectory.

The study of possible needle vibrations shows a periodic response containing not only primary harmonic but also super-harmonics (Fig.13). In the figure the needle trajectory is stable but at the point 1 it begins to vibrate and the trajectory becomes unstable. The vibrations have small amplitudes but as they approach to the tumor shown by no. 2, the needle vibrates and the trajectory becomes unstable.

We can say that it is possible to have a resonance near the tumor. The harmonic vibrations of the needle, the resonance and the phase portrait of the needle trajectory are shown in Fig.14. The simulation shows that the vibrations look as though they contain the primary harmonic and the super-harmonics with very small amplitudes.

4. CONCLUSIONS

The liver is the largest organ in human body with more than 500 identified vital functions for the body health. The liver is susceptible to various diseases, some of which may ultimately evolve to liver tumors. The overall 5-year survival rate of liver cancers is less than 10%, but the number increases to the range of 30% to 60% if the patients are in their early stage and their pathological liver tumors are surgically removable [23]. In other words, early detection is vital for the survival of patients with liver tumors.

The liver tumor therapy by targeted delivery of drugs into the tumor is an innovative technique applied in the case of nonresectable tumors. The present paper refers to the optimization of the collision-free trajectory of the surgical needle who is carrying drugs into the tumoral target, with fulfillment of conditions to not touch the ribs, blood vessels and other tissues and organs in the vicinity of the liver.

The reconstruction of the collision-free workspace and the possible needle insertion areas, as well as the collision-free trajectories are determined by using the particle swarm optimization algorithm. The question on delivering the best and safest care for *no harm* the organs remains to limit the impact of surgical intervention and the modeling which can impact the surgical techniques.

ACKNOWLEDGMENTS

This work was supported by a grant of the Romanian ministry of Research and Innovation, CCCDI – UEFISCDI, project number PN-III-P1-1.2-PCCDI-2017-0221/59PCCDI/2018(IMPROVE), within PNCDI III.

REFERENCES

1. GERVAIS, D.A., ARELLANO, R.S., *Review. Percutaneous Tumor Ablation for Hepatocellular Carcinoma*, American Journal of Roentgenology, 197(4), 789–94, 2011.
2. LIANG, P., WANG, Y., ZHANG, D., YU, X., GAO, Y., NI, X., *Ultrasound Guided Percutaneous Microwave Ablation for Small Renal Cancer: Initial Experience*, The Journal of Urology, 180(3), 844–848, 2008.
3. LIVRAGHI, T., GOLDBERG, S.N., LAZZARONI, S., MELONI, F., IERACE, T., SOLBIATI, L., *Hepatocellular carcinoma: radio-frequency ablation of medium and large lesions*, Radiology, 214(3), 2000, 761–768.
4. SHAOLI LIU, ZEYANG XI, JIANHUA LIU, JING XU, HE REN, TONG LU, XIANGDONG YANG, *Automatic Multiple-Needle Surgical Planning of Robotic-Assisted Microwave Coagulation in Large Liver Tumor Therapy*
5. *PLoS ONE*, 11(3), e0149482, 2016.
6. CRISTINA, S.M., GORKA, G.C., PURIFICACIÓN, G.S., TOMÁS, G.C., CARLOS, P.C., DRECHSLER, K., ERDT, M., LINGURARU, M., OYARZUN, LAURA C., SHARMA, K., SHEKHAR, R., *Computer Science*, 7761, Springer Berlin Heidelberg, 83–90, 2013.
7. BUTNARIU, S., GIRBACIA, F., *Methodology for the Identification of Needles Trajectories in Robotic Brachytherapy Procedure Using VR Technology*, Applied Mechanics and Material, 332, 503–508, 2013.
8. SCHUMANN, C., BIEBERSTEIN, J., BRAUNEWELL, S., NIETHAMMER, M., PEITGEN, H-O, *Visualization support for the planning of hepatic needle placement*, Int J CARS., 7(2), 191–197, 2012.
9. SHAMIR, R., TAMIR, I., DABOOL, E., JOSKOWICZ, L., SHOSHAN, Y., *A Prospective Evaluation of Computer-Assisted Deep Brain Stimulation Trajectory Planning*, Computer Science, 6363, Springer Berlin Heidelberg, 457–464, 2010.
10. CAROLINE VILLARD, L.S., AFSHIN. G., *Radiofrequency ablation of hepatic tumors: simulation, planning, and contribution of virtual reality and haptics*, Biomech. Biomed Engin., 8(4), 215–227, 2005.
11. SEITEL, A., ENGEL, M., SOMMER, C.M., RADELEFF, B.A., VILLAD, C., BAEGERT, C., *Computer-assisted trajectory planning for percutaneous needle insertions*, Med Phys., 38(6), 3246–3259, 2011.
12. ROSENBERG, L.B., *Virtual Fixtures: Perceptual Tools for Telerobotic Manipulation*, IEEE Annual International Symposium, 1993.
13. GLOZMAN, D., SHOHAM, M., *Image-Guided Robotic Flexible Needle Steering*, IEEE Transactions on Robotics, 23(3), 459-467, 2007.
14. ABBOTT, J., MARAYONG, P., OKAMURA, A., *Robotics Research*, *Springer Tracts in Advanced Robotics*, 28, Springer Berlin Heidelberg, 2007.
15. BRIȘAN, C., BOANTĂ, C., CHIROIU, V., *Introduction in optimisation of industrial robots. Theory and applications*, Editura Academiei, 2019.
16. ZHANG, D., WEI, B., IEEE Int. Conf., *Kinematic analysis and optimization for 4PUS-RPU mechanism*, Advanced Intelligent Mechatronics (AIM), 330-335, 2015.
17. CHIROIU, V.**,** BRIȘAN, C., DUMITRIU, D., MUNTEANU, L., *Mechanical Systems and Signal Processing*, 98, 2018, 310-323
18. BRIȘAN, C., VASIU, R.V., MUNTEANU, L., *Transportation Research part C: Emerging Technologies*, 26, 2013, 269-284.
19. CHIROIU, V., MUNTEANU, L., DRAGNE, C., STIRBU, C., *On the diferential dynamic logic model for hybrid systems*, Acta Technica Napocensis, Series: Applied Mathematics and Mechanics, 61(4), 533-538, 2018.
20. MUNTEANU, L., RUGINA, C., DRAGNE, C., CHIROIU, V., *On the robotic control based on interactive activities of subjects*, Proceedings of the Romanian Academy, series A, 2019 (in press).

21. CHIROIU, V., MUNTEANU, L., IOAN, R., DRAGNE, C., MAJERCSIK, L.**,** *Using the Sonification for Hardly Detectable Details in Medical Images,* Scientific Reports, 9, article number 17711, 2019.
22. GRASHOF, F., *Theoretische Mashinenlehre*, Leipzig, 113-118, 1883.
23. XU, Q., LI, Y., *IEEE Int. Conf. Robotics and Biomimetics* (ROBIO'06), 2006, 1169-1174.
24. National Cancer Institute at http://www.cancer.gov/cancerinfo/types/liver [Sep 2008].

Received August 25, 2019